# Cation−Ether Complexes in the Gas Phase: Bond Dissociation Energies of $K^+$(dimethyl ether)$_x$, $x = 1-4$; $K^+$(1,2-dimethoxyethane)$_x$, $x = 1$ and 2; and $K^+$(12-crown-4)

**Michelle B. More,[†] Douglas Ray,*[,‡] and P. B. Armentrout*[,†]**

*Department of Chemistry, University of Utah, Salt Lake City, Utah 84112, and Environmental Molecular Sciences Laboratory, Pacific Northwest National Laboratory, Richland, Washington 99352*

*Received: December 9, 1996; In Final Form: March 21, 1997*[⊗]

Bond dissociation energies (BDEs) of $K^+[O(CH_3)_2]_x$, $x = 1-4$; $K^+[(CH_2OCH_3)_2]_x$, $x = 1$ and 2; and $K^+[c\text{-}(C_2H_4O)_4]$ are reported. The BDEs are determined experimentally by analysis of the thresholds for collision-induced dissociation of the cation−ether complexes by xenon measured using guided ion beam mass spectrometry. In all cases, the primary and lowest energy dissociation channel observed experimentally is endothermic loss of one ligand molecule. The cross section thresholds are interpreted to yield 0 and 298 K BDEs after accounting for the effects of multiple ion−molecule collisions, internal energy of the complexes, and unimolecular decay rates. Trends in the BDEs determined by experiment and recent theoretical *ab initio* calculations are in good agreement, with experimental values being systematically lower than the theoretical values by 5 ± 3 kJ/mol per metal−oxygen interaction. Comparisons to trends in the BDEs for analogous $Li^+$ and $Na^+$ complexes reveal that $Li^+$ is bound less strongly than expected when compared with analogous $Na^+$ and $K^+$ complexes.

## Introduction

Noncovalent interactions between ions and neutral molecules are of fundamental importance in molecular recognition phenomena occurring in complex chemical and biochemical systems.[1] The study of a series of cation−ether complexes composed of different metal cations and a selection of ligands ranging from simple, monodentate ethers to cyclic polyethers provides an opportunity to examine the noncovalent interactions operative in "simple" ion−molecule complexes. Cation−ether complexes are also interesting from a practical point of view. Crown ethers have been proposed for use in new chemical separations technologies[2] and in the development of advanced analytical methods.[3] Computational models capable of reliably predicting ligand selectivity in a variety of condensed phase environments would be valuable tools for the advancement of separations technologies. Such methods are currently under development; however, the development is hindered by a lack of suitable experimental data. One goal of the present work is to provide accurate experimental data to address this deficiency.

Over the past five years, several groups have studied the interactions between crown ethers and alkali metal cations in the gas phase.[4−10] Most work has focused on qualitatively understanding the selectivities of a particular crown ether for the various alkali metal cations. Ion cyclotron resonance and tandem mass spectrometry have been employed to study these systems to obtain selectivities[6,8] via the kinetic method,[11] relative rates of complexation,[5,7] bracketing reactions,[6] and semi-quantitative bond dissociation energy (BDE) measurements.[10] The results of these studies appear to be dependent upon the method of species generation (e.g., fast atom bombardment versus ion−molecule reactions) and method of study (e.g., kinetic method versus bracketing reactions). Dearden et al.[6] surmised that the different ion sources possibly generate energetically and structurally distinct species that alter the selectivities of a given alkali cation toward a crown ether and that the necessary conditions[12] for accurate application of the kinetic method were not being met.

The aforementioned gas phase experiments suggest that quantitative data on well-characterized species would be of value. To this end, we have undertaken the task of determining the BDE of 12-crown-4 (12c4) to the potassium cation using guided ion beam mass spectrometry. In addition to determining this BDE, we have studied the complexes of $K^+$ with smaller acylic ethers**:** dimethyl ether (DME) and 1,2-dimethoxyethane (DXE). The study of these smaller, acylic ethers allows us to better understand the dynamics of dissociation which are of utmost importance in determining accurate BDEs for the larger cyclic polyether complexes. We have recently reported the results of similar experiments on the analogous $Li^+$ and $Na^+$ systems,[13−15] which we compare with the $K^+$ results reported here.

The experimental difficulties involved in accurate BDE determinations for large complexes lie primarily with analyzing the data. These large complexes present a significant new challenge to modeling collision-induced dissociation (CID) data because of their relatively large BDEs and substantial number of vibrational modes. These two features couple synergistically to produce dramatic kinetic shifts (the energy difference between the apparent threshold and actual thermodynamic threshold) even when the initial internal energy of the complexes is taken into consideration. In the following, we analyze our data with several different models of the transition state in an attempt to accurately determine the unimolecular dissociation rate with RRKM theory. This is facilitated by having access to the vibrational frequencies, rotational constants, and geometries of these complexes as calculated by Feller and co-workers.[16,17] This analysis allows determination of accurate BDEs of the $K^+$−ether complexes studied.

## Experimental Section

Complete descriptions of the apparatus and the experimental procedures are given elsewhere.[18,19] The production of $K^+(L)_x$ (L = DME, DXE, and 12c4) complexes is described below. Briefly, ions are extracted from the source, accelerated, and

[†] University of Utah.
[‡] Pacific Northwest National Laboratory.
[⊗] Abstract published in *Advance ACS Abstracts,* May 15, 1997.

S1089-5639(96)04015-7 CCC: $14.00 

focused into a magnetic sector momentum analyzer for mass analysis. Mass-selected ions are retarded to a desired kinetic energy and focused into an octopole ion guide that radially traps the ions. The octopole passes through a static gas cell containing xenon, used as the collision gas, for reasons described elsewhere.[20,21] After exiting the gas cell, product and unreacted reactant ions drift to the end of the octopole, where they are focused into a quadrupole mass filter for mass analysis and subsequently detected by a secondary electron scintillation ion counter using standard pulse counting techniques. Raw ion intensities are converted to absolute cross sections as described previously.[18] Absolute uncertainties in cross section magnitudes are estimated to be ±20%, and relative uncertainties are ±5%.

Ion kinetic energies in the laboratory frame, $E$(lab), are related to center-of-mass (CM) frame energies by $E(\mathrm{CM}) = E(\mathrm{lab})m/(M + m)$, where $M$ and $m$ are the ion and neutral reactant masses, respectively. All energies cited below are in the CM frame unless otherwise noted. Sharp features in the observed cross sections are broadened by the thermal motion of the neutral gas[22] and the distribution of ion energies. The zero of the absolute energy scale and the full width at half-maximum (fwhm) of the ion energy distribution are measured by a retarding potential technique described elsewhere.[18] The fwhm of the ion beam energy distribution was typically between 0.3 and 0.6 eV (lab) for these experiments. The uncertainty in the absolute energy scale is ±0.05 eV (lab).

The complexes are formed in a 1 m long flow tube[19] operating at a pressure of 0.4−0.7 Torr with a helium flow rate of 4000−9000 standard cm$^3$/min. Potassium ions are generated in a continuous dc discharge by argon ion sputtering of a cathode consisting of a carbon steel "boat" containing potassium metal. Complexes are formed by associative reactions with the ligand introduced to the flow tube 5 cm downstream from the dc discharge. Typical operating conditions of the discharge are 3 kV and 30 mA in a flow of 5−15% argon in helium. The flow conditions used in this source provide approximately $10^5$ collisions between the ions and the buffer gas, which should thermalize the complexes both rotationally and vibrationally to 300 K, the temperature of the flow tube. Armentrout and coworkers[23−27] have shown that this assumption is reasonable and no evidence for nonthermal ions was observed in this work.

## Experimental Results

**$K^+(DME)_x$, $x = 1-4$.** Experimental cross sections for the CID of the $K^+(DME)_x$, $x = 1-4$, complexes are shown in Figure 1, parts a−d. The sequential loss of intact DME molecules and ligand exchange with xenon are the major processes observed in these systems over the collision energy range studied, typically 0−10 eV. The cross sections for ligand exchange to form $K^+$(Xe) were small, and thus data for these channels were not collected. The primary (both the lowest energy and dominant) process for all complexes is the loss of a single DME ligand in reaction 1.

$$K^+(DME)_x + Xe \rightarrow K^+(DME)_{x-1} + DME + Xe \quad (1)$$

As $x$ increases, the primary cross section begins to decline more rapidly at higher energies because pathways for the primary product to decompose further become increasingly efficient. All complexes dissociate completely to the bare metal cation at high energies. The shapes of the cross sections and the observed products for dissociation of $K^+(DME)_x$, $x = 1-4$, complexes are very similar to those of the previously studied $Li^+(DME)_x$ and $Na^+(DME)_x$ complexes.[13,15]

**$K^+(DXE)_x$, $x = 1$ and 2.** Experimental cross sections for the CID of the $K^+(DXE)_x$, $x = 1$ and 2, complexes are shown in Figure 2, parts a and b. The cross sections for ligand exchange to form $K^+$(Xe) were small, and thus data for these channels were not collected. The lowest energy and dominant process for all complexes is the loss of a single DXE ligand in reaction 2.

$$K^+(DXE)_x + Xe \rightarrow K^+(DXE)_{x-1} + DXE + Xe \quad (2)$$

The $K^+(DXE)_2$ complex also loses both DXE ligands at elevated energies, but this process is inefficient. The reaction products and cross section shapes observed are similar to those for the CID of $M^+(DXE)_x$, $x = 1$ and 2, where $M^+ = Li^+$ and $Na^+$.[14,15]

**$K^+$(12c4).** Results for the interaction of $K^+$(12c4) with xenon are shown in Figure 3. No products other than $K^+$ and ligand exchange to form $K^+$(Xe) were observed. This behavior is similar to $Na^+$(12c4),[15] but in contrast to the CID results for $Li^+$(12c4).[14] There, the product appearing at the lowest energy did not result from loss of the intact ligand but rather cleavage of the ligand, $Li^+(C_3H_6O_2)$. Other cleavage products, $Li^+(CH_2O)$, $Li^+(C_2H_4O)$, and $Li^+(C_2H_4O_2)$, were also detected at higher energies.

## Thermochemical Analysis

Cross sections are modeled in the threshold region with eq 3

$$\sigma = \sigma_0 \sum g_i (E + E_i + E_{\mathrm{rot}} - E_0)^n / E \quad (3)$$

where $\sigma_0$ is an energy independent scaling factor, $E$ is the relative translational energy of the reactants, $E_0$ is the threshold for reaction of the ground rotational, vibrational, and electronic state, $E_{\mathrm{rot}}$ is the rotational energy of the reactants, and $n$ is an adjustable parameter. The summation is over $i$, which denotes the vibrational states of the complex, $g_i$ is the population of those states ($\sum g_i = 1$), and $E_i$ is the excitation energy of each vibrational state. Because the complexes studied here have many low-frequency vibrational modes, the populations of excited vibrational levels are not negligible at 298 K. The Beyer−Swinehart algorithm[28] is used to calculate the population of the vibrational levels using the frequencies listed in Table 1. Scaled (85, 90, and 100%) vibrational frequencies for all potassium complexes, free 1,2-dimethoxyethane, and free 12c4 are taken from theoretical calculations of Feller and coworkers.[16,17] Frequencies for free DME have been taken from Shimanouchi.[29] The corresponding change in the *average* vibrational energy of the complexes is taken to be an estimate of one standard deviation of the uncertainty in vibrational energy. The form of eq 3 is expected to be appropriate for translationally driven reactions[30] and has been found to reproduce cross sections well in a number of previous studies of both atom−diatom and polyatomic reactions[31,32] including CID processes.[10,21,24] Because the rotational, vibrational, and translational energy distributions are explicitly included in our modeling, the threshold energies determined using eq 3 correspond to 0 K.

In the analysis of $K^+(DME)_x$, $x = 3$ and 4, we use a modified form of eq 3 that accounts for a decline in the cross section for the primary product ion at higher kinetic energies. This model has been described in detail previously.[33] It depends on $E_D$, the energy at which a dissociation channel begins, and $p$, a parameter similar to $n$ in eq 3.

Also considered in the analysis of CID data are the presence of nonthermal ions, pressure effects, and the lifetime of the complex after collisional excitation. Nonthermal ions are

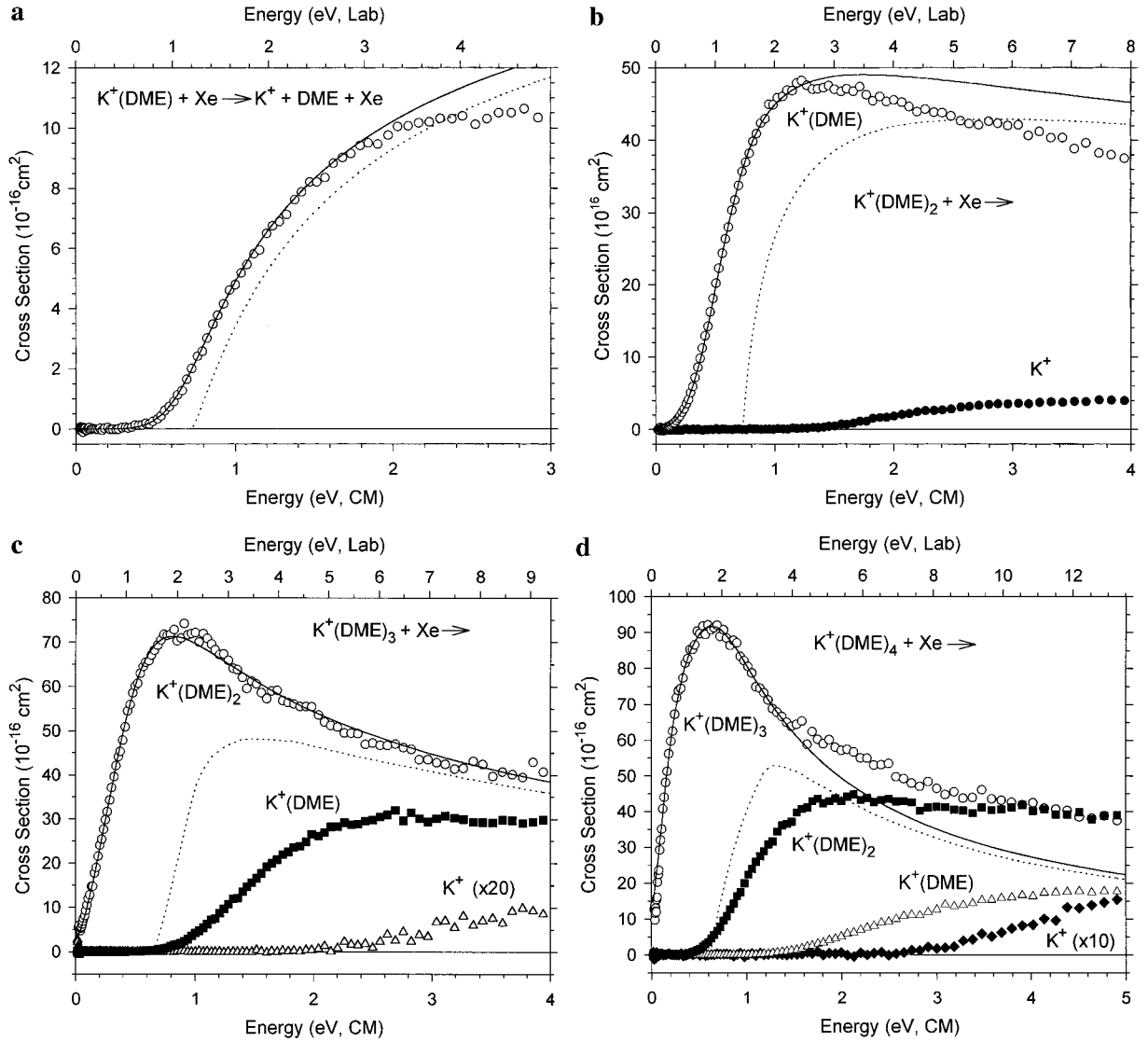


**Figure 1.** Cross sections for reactions of $K^+(DME)_x$ , $x = 1-4$, (parts a−d, respectively) with xenon as a function of kinetic energy in the center-of-mass frame (lower $x$ axis) and the laboratory frame (upper $x$ axis). Open circles show the primary cross sections. The best fits to the data using the model of eq 3 incorporating RRKM modeling for the reactants with an internal temperature of 0 K are shown as dotted lines. Solid lines show these results convoluted over the kinetic and internal energy distributions of the neutral and ionic reactants. Filled circles and open triangles show secondary and tertiary products, respectively.

unlikely because the ions that traverse the 1 m flow tube experience $10^5$ collisions with the buffer gases. Effects due to multiple collisions with Xe are treated by performing the experiments at three different Xe pressures. Dependence on pressure is eliminated, following a procedure developed previously,[34] by linearly extrapolating the cross sections to zero pressure: rigorous single-collision conditions. It is these "zero-pressure" cross sections that are further analyzed.

Lifetime effects are treated by incorporating RRKM theory into eq 3 as previously detailed.[25,35] The additional information needed to implement RRKM theory are the vibrational frequencies of the transition state (TS) associated with the dissociation. Because this TS should be fairly loose, i.e., similar to the products, most of the TS frequencies are those of the products, $K^+(L)_{x-1}$ + L, as listed in Table 1. The remaining TS vibrational frequencies, the transitional frequencies, are those affected most severely as the ligand is removed and are usually hindered rotations, bends, or torsions of the energized molecule. These may not be similar to the product vibrational frequencies and are derived from one of three models of the TS: a tight TS model, a loose TS model, and a phase space limit (PSL) TS model.[15] In all of the models, one $K^+-L$ stretching frequency is chosen as the reaction coordinate and removed. In the tight TS model, the five [two for $K^+$(DME), $K^+$(DXE), and $K^+$(12c4)] remaining frequencies of the $K^+(L)$ reactant are used as the transitional frequencies (listed in boldface in Table 1) without change. In the loose TS model, the transitional frequencies are obtained by dividing these remaining frequencies of the $K^+(L)$ reactant by 2 and 10 to give a range in the looseness of the TS. In the PSL TS model, the transitional modes are assigned as free rotors of the products as described elsewhere.[36]

The entropy of activation, $\Delta S^\dagger$ (the difference in entropy between the reactant and the transition state), is a useful measure of the looseness of a transition state and is also computed for each model of each transition state. These are calculated using the vibrational frequencies given in Table 1 and rotational constants calculated by Feller and co-workers.[16,17] For some of the complexes studied here, it is possible that there is a distribution of energetically similar conformations such that the entropies are not accurate. Unfortunately, a calculation that properly treats such a distribution cannot be performed without molecular parameters for each conformation and accurate relative energy information, neither of which are available. Failure to account for such a possibility is not a major concern

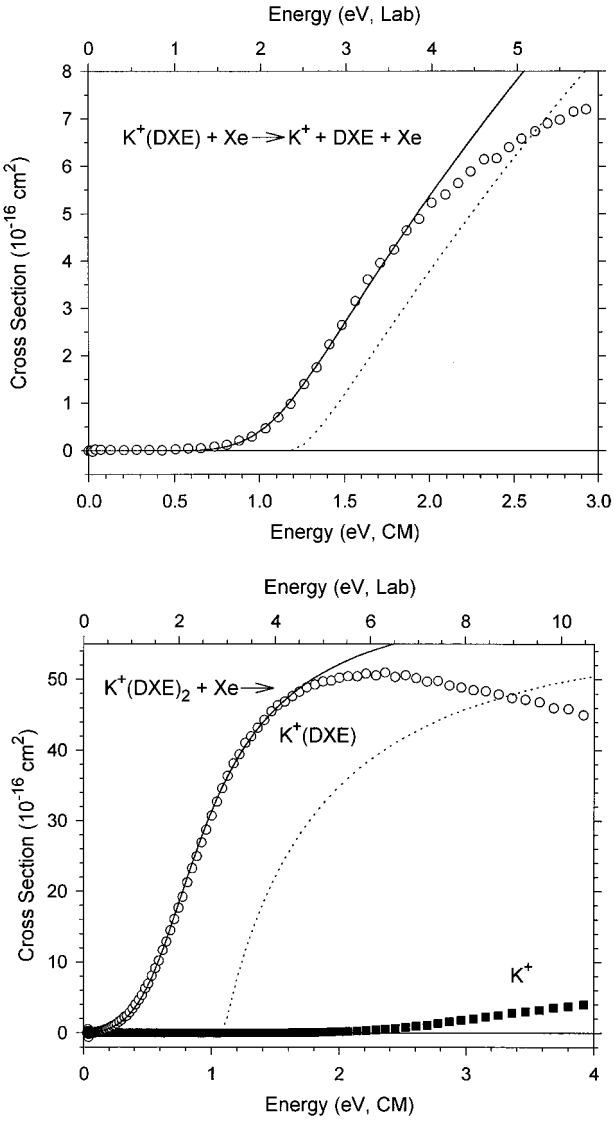


**Figure 2.** Cross sections for reactions of $K^+(DXE)_x$, $x = 1$ and 2 (parts a and b, respectively), with xenon as a function of kinetic energy in the center-of-mass frame (lower *x* axis) and the laboratory frame (upper *x* axis). Open circles show the primary cross sections. The best fits to the data using the model of eq 3 incorporating RRKM modeling for the reactants with an internal temperature of 0 K are shown as dotted lines. Solid lines show these results convoluted over the kinetic and internal energy distributions of the neutral and ionic reactants. Filled circles show the secondary product.

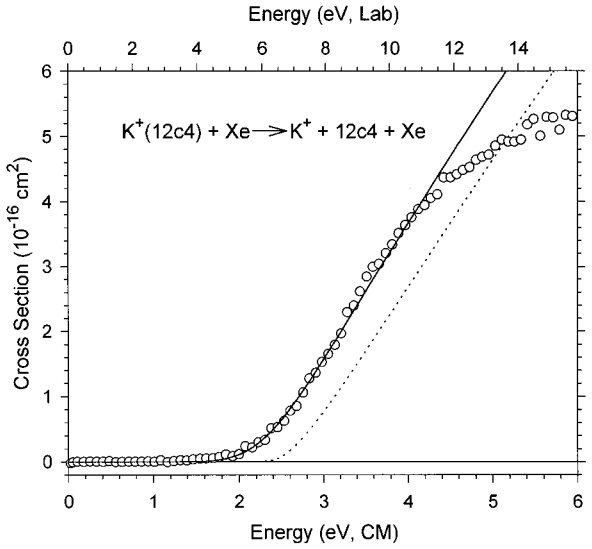


**Figure 3.** Cross sections for the reaction of $K^+(12c4)$ with xenon as a function of kinetic energy in the center-of-mass frame (lower *x* axis) and the laboratory frame (upper *x* axis). Open circles show the primary cross section. The best fits to the data using the model of eq 3 incorporating RRKM modeling for the reactants with an internal temperature of 0 K are shown as dotted lines. Solid lines show these results convoluted over the kinetic and internal energy distributions of the neutral and ionic reactants.

because the primary purpose of the $\Delta S^\dagger$ calculation is as a measure of the *relative* looseness of the transition state for dissociation, which is not affected by the multiple conformations of the complex.

Before comparison with experimental data, eq 3 is convoluted with the kinetic energy distributions of the reactants.[18] The parameters $\sigma_0$, $n$, and $E_0$ are then optimized with a nonlinear least-squares analysis to give the best fit to the data. An estimate of the error in the threshold energy is obtained from variations in $E_0$ for different data sets, variations in the parameter $n$, variations associated with uncertainties in the vibrational frequencies, and the error in the absolute energy scale. Uncertainties listed for $E_0$(PSL), $E_0$(loose), and $E_0$(tight) also include errors associated with variations in the time assumed for dissociation ($10^{-4}$ s) by a factor of 2.5. Uncertainties for $E_0$(loose) and associated $\Delta S^\dagger$ values include variations in the transitional frequencies as mentioned above.

Threshold energies for CID reactions are converted into 0 K BDEs by assuming that $E_0$ represents the energy difference between the reactants and the products at 0 K.[37] This requires that there are no activation barriers in excess of the endothermicity. This is generally true for ion−molecule reactions[31,38] and should be valid for the simple bond fission reactions studied here.[39] This conclusion needs more careful consideration in the case of the multidentate DXE and 12c4 ligands, where the conformation of the ligand changes on going from the lowest energy state of the complex to the lowest energy form of the products. For the DXE and 12c4 ligands, barriers separating these conformations in the absence of the metal ion are likely to be small. We believe that the energy of complexation with the metal ion can overcome any such barriers to rearrangement. In essence, dissociation of the lowest energy conformation of the complex to the products should have no barriers in excess of the bond energy as long as the interaction between the metal cation and the ligand in its lowest energy conformation is attractive at long range. This presumes that barriers between conformations of the complex are less than the binding energy of the metal ion to the ligand; exceptions seem unlikely. Thus, the question of conformations moves from an energetic one to a kinetic one: namely, in the presence of multiple conformations, what is the rate at which the excited complex moves along the lowest energy dissociation path? Given the flexibility of the empirical model used to determine the threshold for dissociation, it seems likely that the true thresholds are still accurately located even if the unimolecular rate constant does not include such an effect explicitly. In the end, comparison of the thermochemistry measured here to theoretical work provides some test of this conclusion. This is discussed below.

Results of the analyses of the cross section data shown in Figures 1−3 are provided in Table 2. To compare the BDEs obtained here with those reported in the literature, the 0 K BDEs can be converted to 298 K BDEs using the standard formulas for the temperature dependence of the enthalpy.[40] Following this method, BDEs for $K^+(DME)_x$, $x = 1-4$, $K^+(DXE)_x$, $x = 1$ and 2, and $K^+(12c4)$ at 298 K can be obtained by adding 0.3, −3.5, −3.6, −3.4, 1.1, −3.3, and 1.9 kJ/mol, respectively, to the 0 K BDEs in Table 2.

**TABLE 1: Vibrational Frequencies and Average Vibrational Energies at 298 K[a]**

| species | $E_{vib}$,[b] eV | frequencies (degeneracies), $cm^{-1}$ |
|---|---|---|
| DME | 0.042 | 203, 242, 418, 928, 1102, 1150, 1179, 1227, 1244, 1452(2), 1464(4), 2817(2), 2925, 2952, 2996(2) |
| $K^+$(DME) | 0.10(0.005) | **80**, **91**, 149, 170, 245, 408, 900, **1080**, 1147, 1174, 1181, 1262, 1452, 1467, 1480, 1484, 1489, 1494, 2898, 2904, 2971, 2972, 2979, 2982 |
| $K^+$(DME)$_2$ | 0.28(0.01) | **1**, **7(2)**, **75**, **76**, 87, 89, 116, 160, 173(2), **244**(2), 406(2), 902, 906, 1085(2), 1148(2), 1177(2), 1182(2), 1264(2), 1452(2), 1469(2), 1481(2), 1484(2), 1488(2), 1495(2), 2894(2), 2901, 2902, 2965(4), 2979(2), 2981(2) |
| $K^+$(DME)$_3$ | 0.47(0.02) | **1(2)**, **5**, **8(2)**, 12, 70, 72(2), 81(2), 87, 92, **149**(2), 176(3), 243(3), 405(3), 906(2), 912, 1088(3), 1148(3), 1182(3), 1183(3), 1264(3), 1452(3), 1469(2), 1471, 1481(3), 1485(3), 1488(3), 1495(2), 1496, 2891(6), 2898(3), 2957(3), 2958(3), 2978(3) |
| $K^+$(DME)$_4$ | 0.65(0.02) | **5(3)**, **11**, **13**, 14(3), 19, 67(3), 73, 77(2), 78(2), 87, 135(2), 142, **178**(3), 179, 240, 241(2), 243, 403(3), 404, 910(3), 917, 1092(4), 1149(4), 1183(4), 1184(3), 1185, 1264(4), 1451(3), 1452, 1470(3), 1472, 1481(2), 1482(2), 1485(4), 1486(2), 1487(2), 1496(3), 1497, 2886(2), 2887(2), 2894(3), 2895, 2950(2), 2951(3), 2952(3), 2979(3), 2980, 2981(3), 2982 |
| DXE | 0.14(0.01) | 68, 110, 118, 144, 209, 229, 319, 383, 487, 814, 955, 1006, 1055, 1140, 1155, 1164, 1167, 1180, 1224, 1232, 1238, 1286, 1357, 1444, 1467, 1478, 1481(2), 1490, 1491, 1509, 1516, 2862, 2863, 2875, 2876, 2893, 2911, 2918(2), 2984, 2985 |
| $K^+$(DXE) | 0.20(0.01) | 40, 102, 103, 124, 136, 153, **192**, **211**, 288, 333, 345, **542**, 835, 853, 1010, 1032, 1099, 1109, 1135, 1163, 1167, 1212, 1227, 1261, 1303, 1398, 1439, 1469, 1474, 1476, 1477, 1488, 1489, 1499, 1501, 2892, 2894, 2899, 2901, 2934, 2944, 2964(2), 2988(2) |
| $K^+$(DXE)$_2$ | 0.48(0.02) | **3**, **7(2)**, 39(2), **73**, 93(2), 101, 105, 117(2), 135, 136, 171, **197(2)**, 212(2), 285, 286, 326(2), 342, 343, 545(2), 841(2), 852, 856, 1013, 1015, 1036(2), 1109(4), 1142(2), 1164(2), 1169(2), 1215(2), 1228(2), 1261(2), 1303(2), 1399(2), 1440(2), 1470(2), 1474(2), 1477(3), 1478, 1487(2), 1489(2), 1499(2), 1501(2), 2885(2), 2887(2), 2893(2), 2895(2), 2925(2), 2935(2), 2953, 2954(3), 2985(4) |
| 12c4 | 0.26(0.02) | 60, 82, 126(2), 146(2), 232, 241(2), 297, 346, 353(2), 363, 460, 517(2), 558, 778, 814(2), 858, 898, 912(2), 933, 1017, 1039(2), 1045, 1094, 1120(2), 1140, 1173, 1176(2), 1184, 1256, 1264(2), 1270, 1286, 1308(2), 1326, 1372, 1391(2), 1409, 1425, 1435(2), 1438, 1482(2), 1483, 1484, 1494(3), 1500, 2857(3), 2858, 2892, 2894(2), 2897, 2935, 2936(2), 2937, 2959, 2960(2), 2963 |
| $K^+$(12c4) | 0.30(0.02) | 61, 109, **119**(2), 135, **146**, **190**(2), 196, 243, 262(2), 283, 332, 349(2), 396, 478, 535(2), 579, 785, 803(2), 846, 888, 905, 908(2), 1027, 1034(2), 1050, 1067, 1112(2), 1134, 1156, 1160(2), 1170, 1253, 1263(2), 1274, 1279, 1303(2), 1317, 1369, 1389(2), 1405, 1428, 1432, 1433, 1484(3), 1485, 1493, 1501(2), 1513, 2891, 2897(2), 2900, 2912, 2915(2), 2920, 2929, 2934(2), 2943, 2968, 2969(2), 2971 |

[a] RHF frequencies are taken from refs 16 and 17 scaled by 0.9. Transitional mode frequencies are in boldface, with the reaction coordinate being the largest of these values. [b] Uncertainties, listed in parentheses, are determined as described in the text.

**TABLE 2: Bond Dissociation Energies at 0 K and Entropies of Activation at 1000 K for $K^+$(DME)$_x$, $x = 1-4$, $K^+$(DXE)$_x$, $x = 1$ and 2, and $K^+$(12c4)[a]**

| species | $E_0$[b] (eV) | $E_0$(PSL) (eV) | $\Delta S^{\ddagger}$(PSL) (J/(mol K)) | $E_0$(loose) (eV) | $\Delta S^{\ddagger}$(loose) (J/(mol K)) | $E_0$(tight) (eV) | $\Delta S^{\ddagger}$(tight) (J/(mol K)) |
|---|---|---|---|---|---|---|---|
| $K^+$(DME) | 0.75(0.05) | 0.76(0.04) | 14 | 0.73(0.05) | 18(19) | 0.73(0.04) | 11 |
| $K^+$(DME)$_2$ | 0.71(0.05) | 0.71(0.05) | −9 | 0.69(0.06) | 59(47) | 0.65(0.05) | 7 |
| $K^+$(DME)$_3$ | 0.65(0.10 | 0.59(0.04) | 4 | 0.63(0.07) | 118(48) | 0.47(0.05) | 12 |
| $K^+$(DME)$_4$ | | 0.52(0.08) | 50 | 0.51(0.07) | 153(47) | 0.20(0.08) | 6 |
| $K^+$(DXE) | 1.32(0.04) | 1.23(0.04) | 39 | 1.21(0.05) | 15(19) | 1.19(0.04) | 11 |
| $K^+$(DXE)$_2$ | 1.20(0.09) | 0.92(0.12) | 24 | 0.94(0.09) | 54(47) | 0.83(0.06) | 3 |
| $K^+$(12c4) | 2.40(0.13) | 1.96(0.12) | 63 | 1.67(0.16) | 41(18) | 1.52(0.12) | 8 |

[a] Uncertainties (one standard deviation) are listed in parentheses. [b] No RRKM lifetime analysis. [c] Data could not be modeled well without incorporating the RRKM lifetime effect into eq 3.

In previous work,[15,35,41] we have found that the PSL TS model generally provides the most accurate thermochemistry (as well as involving the fewest assumptions about the TS[35]), with the loose TS model providing very similar threshold energies. The tight TS values provide very conservative lower limits to the correct thermodynamics, while values obtained with no RRKM modeling provide very conservative upper limits. In the present system, a detailed comparison of the results from these four models with BDEs determined theoretically (see discussion below) confirms these same trends. Thus, the BDEs determined with the PSL TS model and given in Table 3 are the recommended values.

## Discussion

**Comparison with Other Determinations.** The BDE for only one of the complexes examined in this study has been experimentally determined previously. Davidson and Kebarle[42] determined a value of 87 ± 4 kJ/mol for the BDE of $K^+$(DME) at 298 K using high-pressure mass spectrometry. This value is higher than the value of 74 ± 4 kJ/mol reported here. The origins of this discrepancy are unclear. It is clear that the unimolecular dissociation rate of the activated complex does not effect the BDE determined in this work. This is demonstrated by the nearly identical threshold energies determined for $K^+$(DME) with all of the TS models (Table 2). Thus no kinetic shift is evident and our $K^+$(DME) BDE determination does not depend on which transition state model is chosen because the lifetime of the activated complex is less than its flight time (∼100 μs). The possiblity that the conversion to the BDE at 298 K is causing the discrepancy also seems unlikely. As described earlier, the temperature dependence of the enthalpy is calculated with harmonic vibrational frequencies

**TABLE 3: Bond Dissociation Enthalpiees of $K^+(DME)_x$, $x = 1-4$, $K^+(DXE)_x$, $x = 1$ and 2, and $K^+$(12c4) at 298 K in kJ/mol[a]**

| species | $\Delta H_{298}$(PSL) | $\Delta H_{298}$(MP2)[b] |
|---|---|---|
| $K^+(DME)$ | 74(4) | 79 |
| $K^+(DME)_2$ | 65(4) | 64 |
| $K^+(DME)_3$ | 53(7) | 58 |
| $K^+(DME)_4$ | 46(8) | 55 |
| $K^+(DXE)$ | 120(4) | 132 |
| $K^+(DXE)_2$ | 85(12) | 99 |
| $K^+$(12c4) | 191(11) | 196 |

[a] Uncertainties (one standard deviation) are listed in parentheses. [b] 6-31+G* values taken from refs 16 and 17. The enthalpy corrections between 0 and 298 K were determined using MP2 harmonic vibrational frequencies for $K^+(DME)_x$, $x = 1$ and 2, and RHF harmonic vibrational frequencies, scaled by 0.9 for $K^+(DME)_x$, $x = 3$ and 4, $K^+(DXE)_x$, x = 1 and 2, and $K^+$(12c4). Uncertainties in these values are estimated at ±13 kJ/mol, ref 44.

determined at the RHF level of theory. The conversion between temperatures generates a shift of only 0.3 kJ/mol. The enthalpy change required to bring the two $K^+$(DME) BDE determinations into agreement, 13 kJ/mol, cannot be obtained through the use of different, yet reasonable molecular vibrational frequencies or the inclusion of anharmonicity.

Bond dissociation energies of all of the $K^+$ complexes studied here have been calculated by Feller and co-workers [16,17] and are also reported in Table 3. In the work of Feller et al., equilibrium gas phase geometries were optimized using a modified 6-31+G* basis set[43] at the second-order Møller-Plesset perturbation level of theory (MP2) for $K^+(DME)_x$, $x = 1$ and 2, and at the restricted Hartree−Fock (RHF) level of theory for $K^+(DME)_x$, $x = 3$ and 4, $K^+(DXE)_x$, $x = 1$ and 2, and $K^+$(12c4). Correlation corrections were evaluated with frozen-core (the eight valence electrons are included in the correlation), MP2 calculations applied to the optimized geometries. Undesirable basis set superposition errors in the calculated bond energies were estimated with the full counterpoise correction. The theoretical bond dissociation energies are fairly sensitive to the size and completeness of the basis set used, a point recently evaluated for potassium ion−ether complexes in some detail by Feller et al.[44] In that work, it is estimated that BDEs calculated at the MP2 level of theory with the 6-31+G* basis set and counterpoise corrected should be accurate to within ±13 kJ/mol of the complete basis set (CBS) limit.

Agreement between experimental and theoretical values in Table 3 is generally good, within experimental or theoretical error for all complexes. On average, the calculated values are larger than the experimental values by 8 ± 5 kJ/mol (or 5 ± 4 kJ/mol when normalized by the number of oxygen atoms in the ligand). It is certainly feasible that the theoretical values could decrease when BDEs at the complete basis set (CBS) limit are estimated,[14] such that agreement between theory and experiment will improve. For the experimental $K^+$(DXE) BDE to agree more precisely with the theoretical value, the calculated unimolecular dissociation rate would have to be greater. In the limit that no kinetic shift is observed (the fastest possible dissociation rates), the experimental BDE for $K^+$(DXE) does agree with theory (see Table 2), but the use of this model is unjustified for this complex alone and is clearly less accurate for the other complexes studied here and in previous work. As the PSL model is already a very loose TS, it is hard to imagine that a change in TS parameters could allow for the experimental data to be analyzed to yield a $K^+$(DXE) bond energy in precise agreement with theory.

**Bonding and Geometry.** Several trends can be observed in the experimentally determined BDEs (Table 3). The BDEs for the $K^+(DME)_x$ complexes monotonically decrease as $x$ increases. The average drop in the BDEs is 9 ± 3 kJ/mol per additional DME ligand. Likewise, the second DXE ligand is bound 35 kJ/mol more loosely than the first, or 17 kJ/mol per metal−oxygen interaction. This trend is in agreement with theory and conventional ideas of electrostatic ligation of gas phase ions; namely, BDEs decrease with increasing ligation because of increasing ligand−ligand repulsion and increased charge solvation. Not suprisingly, the bidentate complexes, $K^+(DXE)_x$, have greater BDEs than the monodentate complexes, $K^+(DME)_x$, and the tetradentate 12c4 ligand has the largest BDE. As expected, these observations are qualitatively the same as those of the analogous $Li^+$ and $Na^+$ complexes.[13−15]

**TABLE 4: Bond Dissociation Enthalpies of $K^+(DME)_x$, $x = 2$ and 4, $K^+(DXE)_x$, $x = 1$ and 2, and $K^+$(12c4) at 298 K in kJ/mol[a]**

| species | number of oxygens | $\Delta H_{298}$(PSL) |
|---|---|---|
| $K^+(DME)_{1,2}$ | 2 | 139(6) |
| $K^+(DXE)$ | 2 | 120(4) |
| $K^+(DME)_{1-4}$ | 4 | 238(12) |
| $K^+(DXE)_{1,2}$ | 4 | 204(12) |
| $K^+$(12c4) | 4 | 191(11) |

[a] Uncertainties (one standard deviation) are listed in parentheses.

Additional insight into the trends in these BDEs can be obtained by comparing different metal cation ether complexes that contain the same number of carbon and oxygen atoms. $K^+(DME)_2$ and $K^+(DXE)$ form one such series, and $K^+(DME)_4$, $K^+(DXE)_2$, and $K^+$(12c4) comprise another. Table 4 lists these total bond dissociation enthalpies at 298 K. In the first case, we compare the sum of BDEs for removing the first and second DME ligands from $K^+(DME)_2$ to the BDE of $K^+(DXE)$. The difference of 19 ± 7 kJ/mol indicates that the DXE ligand is not bound as strongly as two DME ligands. A similar observation was made for the analogous $Li^+$ and Na complexes[14,15] where differences of 38 ± 26 and 11 ± 8 kJ/mol, respectively, were found. We rationalize this result by noting that the DME ligands are free to align their dipoles perfectly to interact with the $K^+$ ion core and to adjust the metal−ligand bond distances to optimum lengths. In contrast, the DXE ligand is constrained by the geometry of the ligand such that perfect dipole alignment cannot be achieved. Not surprisingly, the sum of BDEs for removing the third and fourth DME ligands from $K^+(DME)_4$, 99 ± 11 kJ/mol, is also larger than the $K^+(DXE)_2$ BDE of 85 ± 12 kJ/mol. This is similar to the analogous lithium and sodium cases[14,15] where the second DXE ligand is bound less strongly than the sum of the third and fourth DME ligands.

Removing all four DME ligands from $K^+(DME)_4$ at 298 K requires 34 ± 17 kJ/mol more than removing the first and second DXE ligands from $K^+(DXE)_2$ and 47 ± 16 kJ/mol more than dissociating $K^+$(12c4). Clearly, the most stable structure in this group is $K^+(DME)_4$. This species has four ligands which can independently align their dipoles and adjust their metal−oxygen ($M^+$−O) distances with the only constraint coming from steric hindrance with neighboring ligands. The next most stable structure is $K^+(DXE)_2$, which is more stable than $K^+$(12c4) because there are fewer constraints on dipole alignment and $M^+$−O distance for the DXE ligands than the 12c4 species.

These conclusions are similar to those drawn by Hay et al.,[45,46] who investigated structural requirements for strain-free metal ion complexation with aliphatic ethers using molecular mechanics and *ab initio* methods. They found that the greatest complex stability was achieved when the metal−oxygen length could be optimized and the atoms surrounding the oxygen atoms were oriented in a trigonal planar geometry. Our results for the analogous $Li^+$ and $Na^+$ complexes[13−15] also support Hay's

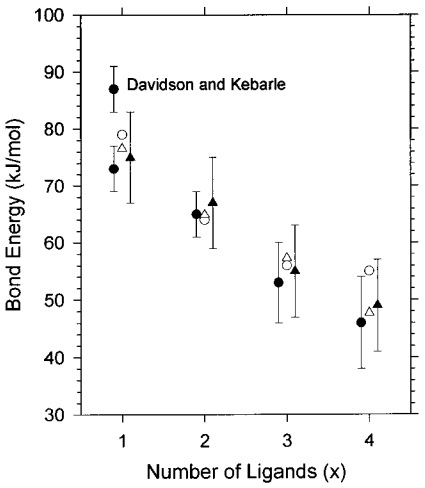


**Figure 4.** Bond energies (in kJ/mol) at 298 K of $(R_2O)_{x-1}K^+-(OR_2)$ where the ligand is dimethyl ether (R = $CH_3$, circles) and water (R = H, triangles) plotted versus *x*. Solid symbols show experimental results, while open symbols exhibit theoretical results. Bond energies for $(DME)_{x-1}K^+-DME$ are taken from Table 3 and ref 42. Bond energies for $(H_2O)_{x-1}K^+-(H_2O)$ are taken from ref 10 (experiment) and ref 48 (theory).

proposal. Clearly, these preferences can be easily achieved by the independent DME ligands, but are constrained by the preorganized DXE and 12c4 ligands.

These results may be used to address the gas phase macrocyclic effect which is evidenced by greater thermodynamic stability of a cyclic ligand complexed to an ion as opposed to an analogous acyclic ligand complexed to the same ion. Dearden et al.[5,7] have observed the gas phase macrocyclic effect by measuring the relative rates of complexation of alkali metal cations with 12-crown-4 and 15-crown-5 and their acyclic analogues, triglyme and tetraglyme. Dearden found that the relative rates for complexation were faster for the crowns than the glymes. Dearden surmised that these findings were a consequence of the preorganized structure of the crown ligand, thus yielding a favorable entropic contribution. Though the ligands employed in this present study consist of a cyclic ligand (i.e., 12c4) and its acyclic analogues (i.e., four DMEs or two DXEs), the present results help confirm Dearden's suggestion, because they show that the acyclic analogues have greater BDEs (enthapic contributions) than the crown ligand. Thus a gas phase macrocyclic effect must exist due to the favorable entropic considerations of the crown ligand.

Comparison of $K^+(DME)_x$ with $K^+(H_2O)_x$ elucidates additional aspects of the bonding. The BDEs of $K^+(H_2O)_x$ , $x = 1-4$, have been determined experimentally by Dzidic and Kebarle[47] using high-pressure mass spectrometry and theoretically by Glendening and Feller[48] using *ab initio* methods. These BDEs are shown in Figure 4 along with experimental and theoretical[16] values for the BDEs of $K^+(DME)_x$, $x = 1-4$. The agreement between experiment and theory for $K^+(H_2O)_x$, $x = 1-4$, is quite good. The BDEs for each set of complexes decrease monotonically as *x* increases. The BDEs of the DME-containing complexes are all slightly smaller than the BDEs of the analogous $H_2O$-containing complexes, with an average difference of 2 ± 1 kJ/mol. This result is comparable to that for the BDEs of $Na^+(DME)_x$, $x = 1-4$, which are smaller than those for $Na^+(H2O)_x$ by an average of 4 ± 3 kJ/mol.[15] In contrast, the BDEs for $Li^+(DME)_x$ are greater than those of $Li^+(H_2O)_x$ for $x = 1$ and 2 and comparable to those of $Li^+(H_2O)_x$ for $x = 3$ and 4.[13] This can be explained by noting that while the dipole moment of $H_2O$ is greater than that of DME, the polarizability of DME is greater than that of $H_2O$. Thus, for

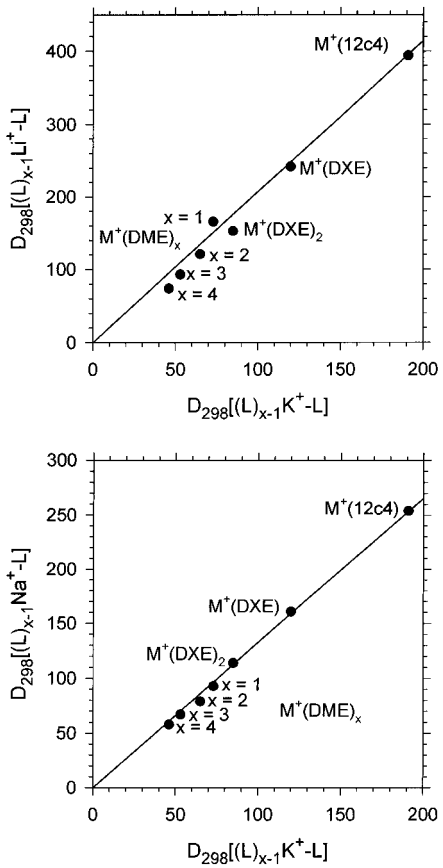


**Figure 5.** Bond energies at 298 K of $K^+$ complexes with dimethyl ether (DME), 1,2-dimethoxyethane (DXE), and 12-crown-4 (12c4) plotted against the BDEs of the analogous $Li^+$ and $Na^+$ complexes (parts a and b, respectively). Bond energies of the $Li^+$ and $Na^+$ complexes are taken from the text (see the Discussion section) and ref 15, respectively.

sufficiently short $M^+-O$ bond lengths, such as those in $Li^+(DME)_x$, $x = 1$ and 2, the ion induced-dipole term dominates the interaction and the $M^+(H_2O)_x$ complexes have smaller BDEs. For longer bond lengths, such as those in $Na^+(DME)_x$ and $K^+(DME)_x$, $x = 1-4$, the ion−dipole term dominates the interaction and the $M^+(H_2O)_x$ complexes have larger BDEs. Further analysis of such alkali cation−ether trends is currently under way for the analogous complexes with $Rb^+$ and $Cs^+$.

**Comparison with Analogous $Li^+$ and $Na^+$ Complexes.** The BDEs at 298 K of the $K^+$ complexes are plotted against those of the analogous $Li^+$ and $Na^+$ complexes in parts a and b of Figure 5, respectively. The CID cross section data for the $Li^+$ complexes[12,14] have been reanalyzed using the PSL TS model, resulting in the following BDEs: 159(10), 121(14), 93(7), and 81(9) for $Li^+(DME)_x$, $x = 1-4$, respectively, and 242(21) and 153(4) for $Li^+(DXE)_x$, $x = 1$ and 2, respectively. For $Li^+$(12c4), the BDE is fairly high and fragmentation of the ligand was competitive with the dissociation of intact 12c4. Therefore, we conclude that the best experimental value for the $Li^+$(12c4) BDE spans the range of the $E_0$(PSL) = 435(20) kJ/mol and $E_0$(tight) = 353(25) kJ/mol, resulting in a BDE of 394(61) kJ/mol at 298 K. While the BDEs obtained with the PSL TS model for the $Li^+$ complexes differ quantitatively from the previously published BDEs obtained with the loose TS model,[13,14] they do not differ qualitatively or alter any of the conclusions drawn in earlier work.

The solid line in each figure is a linear regression of all the BDEs of singly ligated complexes, i.e., of $M^+(L)$, L = DME, DXE, and 12c4, and is constrained to pass through the origin. The slope of the line in Figure 5a is 2.0, indicating that the

singly ligated $Li^+$ BDEs are about twice as strong as the analogous $K^+$ BDEs. Interestingly, the BDEs for the multiligated species, lie below the linear regression line. This pattern suggests that the BDEs of the multiligated $Li^+$ species are somewhat weaker than expected. The natural energy decomposition analysis (NEDA) of Glendening and Feller[13,14,16,17] helps reveal the subtle differences in the bonding of $Li^+$ and $K^+$ to the DME, DXE, and 12c4 ligands. The attractive components per ligand (i.e. the electrostatic, exchange, and charge transfer terms) for both the $Li^+(DME)_x$ and $K^+(DME)_x$ species decrease slightly over the range of $x = 1-4$: 8% and 13%, respectively. However, the repulsive contributions (i.e. distortion of the ligand geometry, deformation of the metal core and ligand charge distributions) vary considerably more. For $Li^+(DME)_x$, the repulsive term per ligand increases about 38% from $x = 1$ to 4, but the $K^+(DME)_x$ repulsive term decreases 9% over this range. Somewhat similar behavior is noted for the DXE ligands. The change in the attractive components for the $M^+(DXE)_x$, $x = 1$ and 2, is 1% and −9%, for M = Li and K, respectively. The repulsive terms for the $Li^+(DXE)_x$ and $K^+(DXE)_x$ species mimic the DME species such that they change by 34% and −4%, for Li and K, respectively. Evidently, the compact lithium cation distorts the charge distribution and geometry of the DME and DXE ligands because of shorter cation−ligand bond lengths. Additionally, the shorter bond lengths in the $Li^+$ complexes significantly increase the ligand−ligand repulsion in the multiligated complexes. These observations point to why the $Li^+$ multiligated BDEs are weaker than expected relative to the $K^+$ BDEs.

The correlation between the BDEs for analogous $K^+$ and $Na^+$ complexes' BDEs, shown in Figure 5b, is very good. On average, the $Na^+$ BDEs are 30% greater than their $K^+$ counterparts, but unlike the $Li^+$ analogues, the multiligated complexes do not distinguish themselves as a group from the singly ligated complexes. Examination of the NEDA results confirms the similar behavior of multi- and singly ligated complexes. The attractive terms of $M^+(DME)_x$ decrease over the range of $x = 1-4$ by 11% and 13%, for M = Na and K, respectively. Likewise, the repulsive terms for both alkali ions decrease by 9% for the range $x = 1-3$ and increase by 9% and 4% (relative to $x = 1$) between $x = 3$ and 4, for M = Na and K, respectively. The bidentate $M^+(DXE)_x$ complexes show more variation for the attractive and repulsive components. The attractive terms for the $Na^+$ and $K^+$ DXE species both decrease by 4% and 9%, respectively, between $x = 1$ and 2. Interestingly, the repulsive terms for $Na^+(DXE)_x$ species increase by 11% from $x = 1$ to 2, whereas those for the $K^+(DXE)$ species decrease by 4%. Apparently, these differences balance themselves such that the bonding in the $K^+$ and $Na^+$ species appears to scale linearly. It also appears that neither $Na^+$ nor $K^+$ induces significant ligand distortion (as noted in the significantly smaller repulsive terms) in comparison to the effects of the $Li^+$ cation.

## Conclusion

Kinetic energy dependent collision-induced dissociation in a guided ion beam mass spectrometer is used to determine the absolute bond energies of potassium cation complexes with one to four dimethyl ether molecules, one and two 1,2-dimethoxyethane molecules, and the 12-crown-4 cyclic polyether. Effects of multiple collisions, internal energies of the complexes, reactant translational energy distributions, and dissociation lifetimes are all considered in the data analysis. Kinetic shifts in the measured thresholds increase with the complexity of the metal−ligand complex and with increasing bond energy. Overall, the results obtained here are comparable to those previously determined for the analogous complexes with $Na^+$.[15] The only significant difference when compared to the analogous $Li^+$ complexes[13,14] occurs for the $M^+$(12c4) complex. No ligand fragmentation channels are observed for M = Na and K, in contrast to the results for $Li^+$(12c4).

The bond energies obtained here experimentally are in good agreement with results of *ab initio* calculations,[16,17] with an average deviation of 5 ± 3 kJ/mol per metal−oxygen interaction. Comparison of complexes containing the same number of metal−oxygen interactions shows that the preorganized multidentate ligands bind less tightly than the cumulative monodentate ligands, an effect attributed to geometric constraints in the former systems. Comparison of the trends in the bond energies between the $Li^+$, $Na^+$, and $K^+$ complexes shows the expected result that the smaller lithium ion has significantly greater BDEs than the sodium ion, which has greater bond energies than the potassium ion. Further, the bond dissociation energies of the $K^+$ complexes are linearly correlated with the analogous $Na^+$ complexes, but deviations are observed for the analogous $Li^+$ complexes. This behavior suggests that the bonding in the $Li^+$ complexes suffers from ligand distortion because ligand−ligand distances are much closer for the compact $Li^+$ cation complexes.

**Acknowledgment.** Funding for this work was provided by the National Science Foundation under Grant No. CHE-9350412 (PBA) and by the Division of Chemical Sciences, Office of Basic Energy Sciences, U.S. Department of Energy (M.B.M., D.R.). Pacific Northwest National Laboratory is a multiprogram national laboratory operated for the U.S. Department of Energy by Battelle Memorial Institute under Contract DE-AC06-76RLO 1830.

## References and Notes

(1) See for example: *Molecular Recognition: Receptors for Cationic Guests*; Gokel, G. W., Ed.; Vol. 1, *Comprehensive Supramolecular Chemistry*; Lehn, J.-M., Ed.; Pergamon Press: New York, 1996.

(2) See for example: Horwitz, E. P.; Dietz, M. L.; Fisher, D. E. *Solvent Extr. Ion Exch.* **1991**, *9*, 1. Moyer, B. A; Delmau, L. H.; Case, G. N.; Bajo, S. Baes, C. F. *Sep. Sci. Technol.* **1995**, *30*, 1047.

(3) See for example: Grate, J. W.; Strebin, R.; Janata, J.; Egorov, O; Ruzicka, J. *Anal. Chem.* **1996**, *68*, 333.

(4) Zhang, H.; Chu, I.-H.; Leming, S.; Dearden, D. V. *J. Am. Chem. Soc.* **1991**, *113*, 7415.

(5) Zhang, H.; Dearden, D. V. *J. Am. Chem. Soc.* **1992**, *114*, 2754.

(6) Chu, I.-H.; Zhang, H.; Dearden, D. V. *J. Am. Chem. Soc.* **1993**, *115*, 5736.

(7) Dearden, D. V.; Zhang, H.; Chu, I.-H.; Wong, P.; Chen, Q. *Pure Appl. Chem.* **1993**, *65*, 423.

(8) Maleknia, S.; Brodbelt, J. *J. Am. Chem. Soc.* **1992**, *114*, 4295.

(9) Brodbelt, J. S.; Liou, C.-C. *Pure Appl. Chem.* **1993**, *65*, 409.

(10) Katritzky, A. R.; Malholtra, N.; Ramanathan, R.; Kemerait, R. C., Jr.; Zimmerman, J. A.; Eyler, J. R. *Rapid Commun. Mass Spectrom.* **1992**, *114*, 2754.

(11) Cooks, R. G.; Kruger, T. L. *J. Am. Chem. Soc.* **1977**, *99*, 1279. McLucky, C. A.; Cameron, D.; Cooks, R. G. *J. Am. Chem. Soc.* **1981**, *103*, 1313.

(12) The necessary conditions for the kinetic method to be useful are (i) competitive reactions must have identical frequency factors, so that their rates are controlled by their activation energies and, (ii) reverse activation energies, which are expected to be small, must be equivalent.

(13) More, M. B.; Glendening, E. D.; Ray, D.; Feller, D.; Armentrout, P. B. *J. Phys. Chem.* **1996**, *100*, 1605.

(14) Ray, D.; Feller, D.; More. M. B.; Glendening, E. D.; Armentrout, P. B. *J. Phys. Chem.* **1996**, *100*, 16116.

(15) More, M. B.; Ray, D.; Armentrout, P. B. *J. Phys. Chem.* **1997**, *101*, 831.

(16) Hill, S. E.; Glendening, E. D.; Feller, D. *J. Chem. Phys.*, submitted for publication.

(17) Glendening, E. D.; Hill, S. E.; Feller, D. *J. Phys. Chem.*, submitted for publication.

(18) Ervin, K. M.; Armentrout, P. B. *J. Chem. Phys.* **1985**, *83*, 166.

(19) Schultz, R. H.; Armentrout, P. B. *Int. J. Mass Spectrom. Ion Processes* **1991**, *107*, 29.

(20) Aristov, N.; Armentrout, P. B. *J. Phys. Chem.* **1986**, *90*, 5135.
(21) Dalleska, N. F.; Honma, K., Sunderlin, L. S.; Armentrout, P. B. *J. Am. Chem. Soc.* **1994**, *116*, 3519.
(22) Chantry, P. J. *J. Chem. Phys.* **1971**, *55*, 2746.
(23) Schultz, R. H.; Armentrout, P. B. *J. Chem. Phys.* **1992**, *96*, 1046.
(24) Schultz, R. H.; Crellin, K. C.; Armentrout, P. B. *J. Am. Chem. Soc.* **1991**, *113*, 8590.
(25) Khan, F. A.; Clemmer, D. C.; Schultz, R. H.; Armentrout, P. B. *J. Phys. Chem.* **1993**, *97*, 7978.
(26) Fisher, E. R.; Kickel, B. L.; Armentrout, P. B. *J. Phys. Chem.* **1993**, *97*, 10204.
(27) Fisher, E. R.; Kickel, B. L.; Armentrout, P. B. *J. Chem. Phys.* **1992**, *96*, 4859.
(28) Beyer, T. S.; Swinehart, D. F. *Comm. Assoc. Comput. Machines* **1973**, *16*, 379. Stein, S. E.; Rabinovitch, B. S. *J. Chem. Phys.* **1973**, *58*, 2438. Stein, S. E.; Rabinovitch, B. S. *Chem. Phys. Lett.* **1977**, *49*, 183. Gilbert, R. G.; Smith, S. C. *Theory of Unimolecular and Recombination Reactions*; Blackwell Scientific Publications: Oxford, 1990.
(29) Shimanouchi, T. *Tables of Molecular Vibrational Frequencies: Consolidated Volume I*; NSRDS-NBS 39; U.S. Government Printing Office, Washington, DC, 1972.
(30) Chesvnavich, W. J.; Bowers, M. T. *J. Phys. Chem.* **1979**, *83*, 900.
(31) Armentrout, P. B. In *Advances in Gas Phase Ion Chemistry*; Adams, N. G., Babcock, L. M., Eds.; JAI: Greenwich, 1992; Vol. 1, pp 83−119.
(32) See for example: Sunderlin, L. S.; Armentrout, P. B. *Int. J. Mass Spectrom. Ion Processes* **1989**, *94*, 149.
(33) Weber, M. E.; Elkind, J. L.; Armentrout, P. B. *J. Chem Phys.* **1986**, *84*, 1521.
(34) Hales, D. A.; Lian, L.; Armentrout, P. B. *Int. J. Mass Spectrom. Ion Processes* **1990**, *102*, 269.
(35) Rodgers, M. T.; Ervin, K. M.; Armentrout, P. B. *J. Chem. Phys.*, in press.
(36) Rodgers, M. T.; Armentrout, P. B. *J. Phys. Chem.*, in press.
(37) Dalleska, N. F.; Honma, K.; Armentrout, P. B. *J. Am. Chem. Soc.* **1993**, *115*, 12125. See Figure 1 of this reference.
(38) Boo, B. H.; Armentrout, P. B. *J. Am. Chem. Soc.* **1987**, *109*, 3459. Ervin, K. M.; Armentrout, P. B. *J. Chem. Phys.* **1987**, *86*, 2659. Elkind, J. L.; Armentrout, P. B. *J. Phys. Chem.* **1984**, *88*, 5454. Armentrout, P. B. In *Structure/Reactivity and Thermochemistry of Ions*; Ausloos, P., Lias, S. G., Eds.; Reidel: Dordrecht, 1987; pp 97−164.
(39) Armentrout, P. B.; Simons, J. *J. Am. Chem. Soc.* **1992**, *114*, 8627.
(40) Chase, M. W.; Davies, C. A.; Downey, J. R.; Frurip, D. J.; McDonald, R. A.; Syverud, A. N. *J. Phys. Chem. Ref. Data* **1985**, *14*, Suppl. 1.
(41) Rodgers, M. T.; Armentrout, P. B. *J. Phys. Chem.*, in press.
(42) Davidson, W. R.; Kebarle, P. *J. Am. Chem. Soc.* **1976**, *98*, 6133.
(43) Hehre, W. J.; Ditchfield, R.; Pople, J. A. *J. Chem. Phys.* **1972**, *56*, 2257.
(44) Feller, D.; Apra, E.; Nichols, J. A.; Bernholdt, D. E. *J. Chem. Phys.* **1996**, *105*, 1940.
(45) Hay, B. P.; Rustad, J. R. *J. Am. Chem. Soc.* **1994**, *116*, 6316.
(46) Hay, B. P.; Rustad, J. R.; Hostetler, C. J. *J. Am. Chem. Soc.* **1993**, *115*, 11158.
(47) Dzidic, I.; Kebarle, P. *J. Chem. Phys.* **1970**, *74*, 1466.
(48) Glendening, E. D.; Feller, D. *J. Phys. Chem.* **1995**, *99*, 3060.